Published in final edited form as:
*Anal Biochem*. 2007 February 15; 361(2): 218–225. doi:10.1016/j.ab.2006.11.011.

# Quantitative continuous assay for hyaluronan synthase

**Joanne C. Krupa**[a], **David Shaya**[b], **Lianli Chi**[c], **Robert J. Linhardt**[c], **Miroslaw Cygler**[b,d], **Stephen G. Withers**[e], and **John S. Mort**[a,f,*]

[a] Joint Diseases Laboratory, Shriners Hospital for Children, Montreal, Que., Canada H3G 1A6

[b] Department of Biochemistry, McGill University, Montreal, Que., Canada H3G 1Y6

[c] Rensselaer Polytechnic Institute, Biotechnology Center 4005, Troy, NY 12180, USA

[d] Biotechnology Research Institute, NRC, Montreal, Que., Canada H4P 2R2

[e] Department of Chemistry, University of British Columbia, Vancouver, BC, Canada V6T 1Z1

[f] Department of Surgery, McGill University, Montreal, Que., Canada H3G 1A4

## Abstract

A rapid, continuous, and convenient three-enzyme coupled UV absorption assay was developed to quantitate the glucuronic acid and *N*-acetylglucosamine transferase activities of hyaluronan synthase from *Pasteurella multocida* (PmHAS). Activity was measured by coupling the UDP produced from the PmHAS-catalyzed transfer of UDP-GlcNAc and UDP-GlcUA to a hyaluronic acid tetrasaccharide primer with the oxidation of NADH. Using a Xuorescently labeled primer, the products were characterized by gel electrophoresis. Our results show that a truncated soluble form of recombinant PmHAS (residues 1–703) can catalyze the glycosyl transfers in a time- and concentration-dependent manner. The assay can be used to determine kinetic parameters, inhibition constants, and mechanistic aspects of this enzyme. In addition, it can be used to quantify PmHAS during purification of the enzyme from culture media.

### Keywords

*Pasteurella multocida* hyaluronan synthase; UDP-glycosyltransferase; Glycosaminoglycan; Hyaluronan synthase

Glycosaminoglycans (GAGs)[1] are naturally occurring biopolymers consisting of disaccharide repeats that often are N- and/or O-sulfated. There are four main classes of GAGs: heparin and heparan sulfate, chondroitin and dermatan sulfate, keratan sulfate, and hyaluronic acid (HA). HA, which consists of the disaccharide repeat GlcUA(β1–3)-GlcNAc(β1–4), plays an important role in normal health and development [1] as well as in inflammation [2], wound repair [3], and cancer pathology [4,5]. GAGs, and in particular HA, have been used therapeutically (reviewed in Ref. [6]) in the treatment of arthritis [7] and cancer [8]. However, in some bacteria, HA forms part of the external capsule [9],



* Corresponding author. Fax: +1 514 842 5581. jmort@shriners.mcgill.ca (J.S. Mort).

thereby contributing to pathogenicity [10,11]. Hyaluronan synthases (HASs) are the glycosyltransferases responsible for the biosynthesis of HA. These enzymes are dual-action

[1]*Abbreviations used:*

| | |
|---|---|
| GAG | glycosaminoglycan |
| HA | hyaluronic acid |
| Glc | D-glucose |
| GlcUA | D-glucuronic acid |
| GlcNAc | *N*-acetyl-D-glucosamine |
| HAS | hyaluronan synthase |
| PmHAS | *Pasteurella multocida* hyaluronan synthase |
| FACE | Xuorophore-assisted carbohydrate electrophoresis |
| ANDA | 7-amino-1,3-naphthalene disulfonic acid |
| PEP | phosphoenolpyruvate |
| NADH | β-nicotinamide adenine dinucleotide-reduced form |
| HAase | hyaluronidase |
| UDP | uridine 5′-diphosphate |
| UDP-Glc | uridine 5′-diphosphate D-glucose |
| UDP-GlcNAc | uridine 5′-diphosphate *N*-acetyl-D-glucosamine |
| UDP-GlcUA | uridine 5′-diphosphate D-glucuronic acid |
| TRU | turbidity-reducing unit |
| IPTG | isopropyl β-D-1-thiogalactopyranoside |
| EDTA | ethylenediaminetetraacetic acid |
| $HA_4$ | hyaluronic acid tetrasaccharide |
| ESI–MS | electrospray ionization–mass spectrometry |
| TFA | trifluoro-acetic acid |
| DTT | dithiothreitol |
| $NAD^+$ | β-nicotinamide adenine dinucleotide |
| $K_{M,\ app}$ | apparent Michaelis–Menten constant |
| $K_{i,\ app}$ | apparent inhibition constant |
| PK | pyruvate kinase |
| L-LDH | L-lactate dehydrogenase |

glycosyltransferases [12-14] that bind both UDP-GlcUA and UDP-GlcNAc in two separate active sites that alternately catalyze the formation of two different glycosidic bonds in the presence of either $Mg^{2+}$ or $Mn^{2+}$ [15].

Although HASs have been characterized enzymologically [12,13,15-22], very little is known about their structure and mechanism. One of the reasons for the limited amount of mechanistic information is the lack of a continuous and convenient activity assay. The current benchmark assay [15,23] relies on the incorporation of $^{14}C$ or $^{3}H$ from UDP-[$^{14}C$]GlcUA or UDP-[$^{3}H$]GlcNAc into higher molecular weight oligomers and the use of paper chromatography to separate the products from the starting materials [24]. Similarly, Malinowski and coworkers [25] developed a glass Wber Wlter paper assay using a radioactive substrate to screen large numbers of samples quickly, and a comparable assay allowed Larjava and coworkers [26] to measure the HAS activity in skin biopsies. Other in vitro assays (reviewed in Ref. [27]) involve metabolic labeling with [$^{3}H$]glucosamine or [$^{3}H$]acetate. Although assays employing radioactive substrates have the advantage of sensitivity, the materials are expensive and require time-consuming steps to separate the unreacted products. Here, we report an inexpensive, continuous, and convenient three-enzyme coupled UV absorption assay for *Pasteurella multocida* hyaluronan synthase (PmHAS) adapted from that developed for other glycosyltransferases [28-31]. The basis for the assay is that pyruvate kinase can employ UDP instead of ADP and thus can be used in the quantification of UDP liberated as a product of the HAS reaction [32]. To our knowledge, the current assay is the Wrst reported example, where this approach is used for a glycosyltransferase, involving a three-substrate coupling, that is, the catalyzed transfer of GlcNAc and GlcUA from UDP-Glc-NAc and UDP-GlcUA to the nonreducing end of HA during the process of chain extension. The assay can detect the enzyme in crude recombinant protein preparations and also can be useful as a tool for detailed mechanistic studies.

## Materials and methods

### Materials

Fermentation-generated ultrapure HA was a generous gift from Clear Solutions Biotech (Stony Brook, NY, USA). HA used for the generation of the Xuorophore-assisted carbohydrate electrophoresis (FACE) HA primer was a generous gift from Toshihiko Toida (Chiba University, Japan). Size exclusion chromatography media BioGel P-2 was purchased from Bio-Rad (Hercules, CA, USA). Sephadex G-50 (medium), Sephadex G-25 (superfine), 7-amino-1,3-naphthalenedisulfonic acid (ANDA), UDP-GlcUA, UDP-GlcNAc, UDP-Glc, phosphoenolpyruvate (PEP), NADH, L-lactate DH (type XI, 915 U/mg solid, rabbit muscle), pyruvate kinase (type III, 283 U/mg solid, rabbit muscle), and bovine testicular hyaluronidase (HAase, type 1-S, 608 U/mg solid, EC 3.2.1.35) were purchased from Sigma–Aldrich (Milwaukee, WI, USA). *Streptomyces hyalurolyticus* HAase (163 turbidity-reducing units [TRUs]/ampoule, EC 4.2.2.1) was obtained from Calbiochem (San Diego, CA, USA).

### Cloning, expression, and purification of recombinant PmHAS

The gene coding for PmHAS as a soluble form (residues 1–703) was amplified by standard PCR techniques from the genomic DNA of *P. multocida* type A strain P-1059 using the following forward and reverse primers: AAA-AAA-CAT-ATG-AAT-ACA-TTA-TCA-CAA-GCA-ATA-AAA-GC and AAA-AAA-GGA-TCC-TTA-AAT-ATC-TTT-TAA-GAT-ATC-AAT-CTC-TTC-TTG. These primers introduced *Nde*I and *Bam*HI restriction sites (underlined), respectively. The resulting DNA fragment was cloned into a modified pET15b vector (Novagen, Madison, WI, USA), coding for an N-terminal His8 tag followed by a thrombin cleavage site, all under the control of the T7 promoter. The DNA was transformed into the *Escherichia coli* expression strain BL21(DE3), and the truncated protein was expressed according to manufacturer's protocol. Briefly, the cells were grown at 37 °C with shaking (250 rpm) to an $OD_{600}$ of 0.6 in 1L of LB media containing 50 μg/ml of ampicillin. Then the culture was incubated at 30 °C for approximately 10 min, after which time the cells were induced with 1 mM IPTG for 3 h. The cells were harvested at 6000*g* for 15 min at 4 °C. The pellet was stored frozen at −80 °C. For enzyme purification, the frozen cell pellet was suspended in 50 ml of 20 mM Tris–HCl (pH 8.0) containing a complete cocktail of EDTA-free protease inhibitors (Roche), 1 mg/ml of lysozyme, and 25 U/ml of benzonase nuclease (Novagen). The suspension was kept on ice for 30 min, and then the cells were disrupted by sonication. Triton X-100 was added to a final concentration of 1% (v/v), and the mixture was stirred gently for 1.5 h at 4 °C followed by centrifugation at 13,000*g* for 40 min at 4 °C. The supernatant was dialyzed (regenerated cellulose MW cutoff 12,000–14,000, Fisher) at 4 °C against 2 × 4L of 50 mM Na phosphate (pH 8.0), 300 mM NaCl, and 10 mM imidazole and then was clarified by centrifugation (2 × 3000*g*, 20 min, 4 °C). The His8-tagged protein was purified by batch elution on an Ni-NTA agarose column (Qiagen) under native conditions. The desired fractions were pooled and dialyzed against 2 × 4L of 10 mM Hepes (pH 7.5) at 4 °C to give a final stock solution of 30 μM enzyme. Here 1 L of LB media yielded approximately 50 mg of purified $PmHAS^{1–703}$ as estimated using the extinction coefficient 85,500 $M^{-1}$ $cm^{-1}$ [33].

### Generation and purification of hyaluronic acid tetrasaccharide

The hyaluronic acid tetrasaccharide ($HA_4$) used in the kinetic studies was prepared as described by D'Auria and coworkers [34]. HA (60 mg, 2.17 MDa) was dissolved in 30 ml of 20 mM NaOAc (pH 5.6) and 150 mM NaCl over 72 h at 4 °C with gentle rocking followed by equilibration to 30 °C. Bovine testicular HAase (60 mg, 0.603 TRU/mg, in 1 ml of the above buffer) was added and the mixture was allowed to rock gently for 32 h, after which time the same amount of bovine testicular HAase was added and the mixture was rocked at 30 °C for a further 4 days. Then an additional 30 mg of HAase was added in a volume of 0.5 ml and the solution was left to stir for an additional 48 h. Then the mixture was heated to 100 °C for 10 min, followed by cooling to 0 °C. The solutions were clarified by repeated centrifugation (3 × 3000*g*, 20 min). The solutions were lyophilized, and the combined brown solid was resuspended in a total volume of 500 μl of sterile $H_2O$. Before loading onto a Bio-Gel P2 Gel Fine column (168 × 1.5 cm), the sample was centrifuged at 16,000*g* for 10 min at 4 °C. The column was eluted with $H_2O$ at a flow rate of 10 ml/h, and 1-ml fractions were collected. The fractions (samples 159–172) containing sugars were identified using a

colorimetric assay for carbohydrates containing an *N*-acetyl group [35,36]. Mass spec [high-resolution electrospray ionization–mass spectrometry (ESI–MS)] run in negative mode yielded two major peaks of *m*/*z* 775.2 and 797.2 corresponding to the tetrasaccharide and its mono sodium salt, respectively. Purity was determined by reverse-phase HPLC using a YMC CombiScreen ODS-AQ (S-5 μM particle size, 50 × 4.6 mm i.d. column, Waters, Beverly, MA, USA). The product eluted at 5.35 min using a linear gradient of 5–50% aqueous acetonitrile containing 0.1% trifluoroacetic acid (TFA) over 5.5 min at a flow rate of 3 ml/min monitoring at 220 nm. Purity was estimated at 90%, and 31 mg of a uniform sample of $HA_4$ was obtained.

### PmHAS assay protocol

Kinetic measurements were carried out, in a total volume of 100 μl, using a Beckman DU-640 spectrophotometer equipped with a thermostated cuvette holder. All measurements were carried out at 25 °C in 20 mM Hepes (pH 7.5), 5 mM $MnCl_2$, 50 mM KCl, and 5 mM dithiothreitol (DTT) that was freshly prepared prior to use. All substrates and enzymes were diluted in the above buffer with the following noted exceptions: $HA_4$ primer was dissolved in water, and PmHAS was diluted in 10 mM Hepes (pH 7.5, stock solution). The decrease in UV absorbance from the conversion of NADH to $NAD^+$ was monitored at 340 nm. A plot of UV absorbance versus [NADH] was linear in the range of 0–0.46 mM or 0–2 absorbance units. Initial rates were calculated after an initial equilibration/lag period of 3 min. All kinetic runs were performed in duplicate. Control experiments were carried out omitting the substrate under study (either UDP-GlcUA, UDP-GlcNAc, or $HA_4$) from the reaction vessel. These individual background rates were subtracted from the values obtained when all three substrates were present in the cuvette. When measuring the apparent Michaelis–Menten constant ($K_{M,\,app}$) for one substrate, the concentrations of the other two substrates were held constant and near saturating (≥4 $K_{M,\,app}$). The kinetic parameter $K_{M,\,app}$ was obtained by Wtting the initial rates to the standard Michaelis–Menten equation using a nonlinear regression program (GraFIT, version 5.0.11, Erithacus Software). Inhibition by UDP-Glc was measured by varying its concentration from 0 to 31 mM while keeping the concentration of UDP-GlcNAc, UDP-GlcUA, and $HA_4$ constant at $0.5K_{M,\,app}$. The apparent inhibition constant ($K_{i,\,app}$) was determined by applying linear regression to a Dixon plot of 1/v versus [UDP-Glc] using GraFIT software. Rates were obtained at 610% NADH oxidation. A representative kinetic assay was performed as follows. To a 0.1-ml quartz cuvette pre-equilibrated at 25 °C with 20 mM Hepes (pH 7.5), 5 mM $MnCl_2$, 50 mM KCl, and 5 mM DTT was added 0.7 mM PEP, 7.5 U pyruvate kinase, 140 μM NADH, 15 U L-LDH, 56 μM UDP-GlcUA, 2.6 mM UDP-GlcNAc, and 3.6 mM $HA_4$. The reaction was initiated by the addition of 4 μl PmHAS from the stock solution in 10 mM Hepes (pH 7.5) to bring the total reaction volume to 100 μl.

### Synthesis of ANDA-labeled $HA_4$

ANDA-labeled $HA_4$ was prepared according to the method of Starr and coworkers [37]. $HA_4$ (1.0 mg) was incubated in ANDA solution [25 mg ANDA in 500 μl of 15% (v/v) HOAc] for 1 h, followed by the addition of 500 μl of a 1-M $NaBH_3CN$ solution. The mixture was stirred for 12 h at 45 °C. $HA_4$-ANDA was purified on a Sephadex G-25 column and freeze-dried.

$^1$H NMR and ESI–MS were used to confirm the structure of $HA_4$-ANDA. ESI–MS run in negative mode exhibited a distribution of molecular ions of the type $[M-(x+1)H+xNa]^-$, where M represents the fully protonated form of the tetrasaccharide (*m*/*z* 1062.1, 1084.0, 1106.1 corresponding to $x = 0, 1, 2$). ESI–MS run in the positive mode exhibited molecular ions of the types $[M+H]^+$ (*m*/*z* 1064.1) and $[M-yH+(y+1)Na]^+$ (*m*/*z* 1086.1, 1108.1, 1130.0, 1152.0, 1174.0 corresponding to $y = 0, 1, 2, 3$, and 4).

$^1$H NMR (500 MHz, $D_2O$) revealed Wve aromatic protons at $\delta$ 7.21 (1H, dd, $J = 9$ Hz, $J = 2.2$ Hz), 7.64 (1H, d, $J = 2.2$ Hz), 7.93 (1H, d, $J = 9$ Hz), 8.307 (1H, d, $J = 7.9$ Hz), 8.311 (1H, d, $J = 7.9$ Hz), and the absence of the anomeric proton at 5.16 ppm found in the NMR spectrum of $HA_4$.

### Synthesis of HA polysaccharides

The reaction was carried out in 20 mM Hepes (pH 7.5), 5 mM $MnCl_2$, 5 mM DTT, and 50 mM KCl at 22 °C for 16 h in the absence of light and in a total volume of 10 μl. The reaction mixture contained 30 nmol of both UDP-GlcUA and UDP-GlcNAc and 3 nmol of $HA_4$-ANDA. The reaction was initiated by the addition of unpurified recombinant PmHAS to an overall estimated concentration of 2.5 μg/ml.

### Preparation of oligomers from HA

Samples of elongated $HA_4$-ANDA, prepared in the 16-h reaction (described above), were adjusted to pH 4.7 by the addition of 1 μl of 1.0 M NaOAc. The mixture was boiled for 5 min, and 1 μl of a 400-TRU/ml solution of *Streptomyces* or bovine testicular HAase was added to bring the final HAase concentration to 0.4 U. The reaction mixture was incubated at 37 °C for 23 h.

### Fluorophore-assisted carbohydrate electrophoresis

FACE was carried out as described previously [38-40] except that a Mini Protean II (Bio-Rad) electrophoresis apparatus was employed and a magnetic stirring bar was used to circulate the running buffer [0.192 M glycine and 25 mM Tris (pH 8.4)], which was cooled to 4 °C prior to the start of the electrophoresis and was maintained at that temperature during the entire experiment. The running and stacking gels were composed of 27 and 5% acrylamide, respectively. The gel was 1.5 mm thick and 5.5 cm long. The 10- and 12-μl samples (from a synthesis or digestion reaction, respectively) were mixed with 2 μl of 50% (w/v) sucrose, and the gels were run for 165 min at 200 V with a starting current of 11 mA. The starting materials and products were visualized by using a longwave UV lamp.

## Results and discussion

PmHAS transfers GlcNAc and GlcUA from UDP-Glc-NAc and UDP-GlcUA to the nonreducing end of HA during the process of HA chain extension (reviewed in Refs. [23,41]), releasing UDP as a by-product. This newly adapted assay for PmHAS activity relies on reacting the released UDP (Eq. (1) in Fig. 1) with PEP in the presence of pyruvate kinase (PK, Eq. (2) in Fig. 1). Then the product pyruvate (Eq. (2)) is reduced to L-lactate with concomitant oxidation of NADH to $NAD^+$ (Eq. (3) in Fig. 1) in the presence of L-

lactate dehydrogenase (L-LDH). NADH absorbs moderately at 340 nm ($\varepsilon = 5740\ M^{-1}\ cm^{-1}$) compared with $NAD^+$ ($\varepsilon = 7.8\ M^{-1}\ cm^{-1}$), thereby providing the basis for a signal decrease assay for HAS. In this coupled system, a linear dependence between the rate of NADH oxidation and the PmHAS concentration is obtained.

As a first validation step, confirmation was obtained that components of the assay associated with Eqs. (2) and (3) in Fig. 1 were not rate limiting. Thus, increasing the [L-LDH], [PK], and [PEP] from 150 U/ml, 75 U/ml, and 0.7 mM to 5000 U/ml, 3750 U/ml, and 3.5 mM, respectively, did not have any effect on rates. Also, increasing [NADH] by two-fold did not alter the observed rates. Setting [NADH] at 140 μM not only kept the assay in the linear range of NADH absorbance but also maintained the absorbance at less than 1.0, making the assay suitable to most UV–Vis spectrophotometers. Therefore, the final concentrations of the commercially available components of Eqs. (2) and (3) added in the standard assay mixture were set as follows: 0.7 mM PEP, 75 U/ml PK, 140 μM NADH, and 150 U/ml L-LDH.

The initial HA fragment that elongates during the reaction can be prepared easily by digesting full-length HA with bovine testicular HAase [34]. HA digested by bovine testicular HAase leaves GlcUA at its nonreducing end [23]. When screening crude protein preparations for HAS activity, partially digested HA fragments can be used without any purification. However, for detailed kinetic analysis where the concentration of the primer is important, purified HA tetrasaccharide was used and was shown to be a suitable substrate for the recombinant enzyme. An initial lag period between 0 and 3 min usually was observed. This lag was not observed if the reaction illustrated in Eq. (1) in Fig. 1 was by-passed by starting the reaction with the addition of 15–300 μM exogenous UDP. A similar lag period was also noted by Tlapak-Simmons and coworkers [42] for *Streptococcal* HAS. As the glycosyltransferase reaction proceeds, the HA chain extends. In addition, as the time course continues, a faster rate is observed. This increase in absorbance per minute may be explained in part by the extended HA chain becoming a progressively better substrate for PmHAS, resulting in a faster reaction rate. For this reason, we selected the rate between 3 and 4 min for the evaluation of kinetic parameters, although these did not change appreciably when other time intervals were used. Determining the initial rate before the steady state is established ensures that the rates measured correspond more closely to the transfer of *N*-acetyl-glucosamine to $HA_4$ followed by glucuronic acid to the newly formed $HA_5$ and also minimizes the variation in the HA concentration.

As a dual transferase, PmHAS transfers both GlcNAc and GlcUA to the nonreducing end of the growing HA chain in an alternating fashion starting with the addition of GlcNAc to the HA tetrasaccharide [23]. Incorporating only UDP-GlcNAc into the reaction mixture containing the HA tetrasaccharide results in a substantial rate in the absence of UDP-GlcUA. This rate is nearly 50% of the maximal observed working at $\geq 4K_{M,\,app}$ for all three substrates. Thus, to determine the $K_{M,\,app}$ for UDP-GlcUA, it was necessary to subtract the two-substrate rate from all runs. As expected, incorporating just UDP-GlcUA and $HA_4$ into the reaction mixture showed only minimal background drift.

Control reactions were carried out to ensure that the measured transferase activity was due to the activity of the recombinant soluble enzyme and not to any other protein present in the crude mixture. Protein collected from the soluble fraction of sonicated BL21(DE3) cells yielded activity only when the cells were induced with IPTG. When the cells were not induced or when they contained only empty vector, rates equivalent to background were observed. When extracts of induced cells were assayed in the presence of a 2MDa intact HA polymer rather than $HA_4$, no rate over background was observed because the effective concentration of the nonreducing end is negligible. In addition, the total absence of HA did not lead to NADH oxidation. Thus, the rate observed originated solely from the presence of recombinant PmHAS even in crude preparations, confirming that the crude enzyme activity can be coupled to the oxidation of NADH in a concentration-dependent manner. This indicates that multiple biological samples could be screened quickly and efficiently for enzymatic activity.

The assay has also been used for detailed kinetic and mechanistic studies. Fig. 2 shows how the rate of NADH oxidation at constant near-saturating substrate concentrations ($4K_{M,\,app}$) was used to estimate the detection limit. A linear response of rate versus [PmHAS] resulted. Under these conditions, the assay has a maximal rate of −0.061 abs/min. Reproducible rates were detected down to 75 nM (~6.2 μg/ml) of purified PmHAS (Fig. 2). The detection limit was taken as 10% of this maximal rate. Because on purification of PmHAS an approximately 11-fold reduction in enzymatic activity was observed [18], we expect that the detection limit is significantly higher in crude enzyme preparations, thereby facilitating the detection of PmHAS in biological samples using this assay.

To characterize the elongated HA chains generated by PmHAS activity, we used FACE in conjunction with an $HA_4$ primer labeled at the reducing end by reaction with ANDA (Fig. 3). These products can be visualized easily by longwave UV with a detection limit estimated to be 0.05 nmol on a 1.5-nm thick 27% acrylamide gel. Consistent with the 90% purity of the $HA_4$-ANDA preparation, on electrophoresis a major band was observed along with a minor component of lower mobility corresponding to a small amount of contaminating $HA_6$-ANDA (Fig. 4, lanes 1 and 2). In the presence of cell lysates containing PmHAS and UDP sugars, this fluorescent primer elongated to form higher molecular weight products, as indicated by the presence of bands with lower migratory potential when compared with the primer alone (Fig. 4, lanes 4 and 5). By band counting, we estimate that oligosaccharides in the range of 12–28 saccharide units are produced and that, given the close spacing of the bands, both odd and even oligomers are present. Cell lysates from cells transformed with the vector alone failed to generate bands of lesser mobility, and those from non-induced cultures showed only a small amount of $HA_8$-ANDA (Fig. 4, lane 3), suggesting low-level leakage of PmHAS expression. The same was true for samples containing either no UDP sugars or no PmHAS (Fig. 4, lane 1). Incubation of these high-molecular weight products with either *Streptomyces* (Fig. 4, lane 6) or bovine testicular HAase (Fig. 4, lane 7) produced fragments of greater mobility. Although not migrating to the same baseline position as the primer alone, the fragments were smaller in size than the starting material, predominantly from $HA_6$-ANDA and $HA_8$-ANDA in the case of *Streptomyces* HAase but from $HA_8$-ANDA to $HA_{18}$-ANDA for testicular HAase. It is possible that in the presence of the large bulky

Xuorophore (ANDA), these HAases are not able to readily digest the HA polymer back to $HA_4$-ANDA. It is known that the testicular enzyme is not as specific as the *Streptomyces* HAase with respect to substrate specificity, cleaving both chondroitin sulfate and HA, whereas the *Streptomyces* enzyme will cleave only HA (reviewed in Ref. [43]). The multiple bands observed in lanes 4 and 5 (Fig. 4) of the FACE gel are also consistent with PmHAS catalyzing the polymerization in a nonprocessive manner [44]; that is, the enzyme binds the HA fragment, elongates the chain, and then releases it. Then the cycle repeats.

Finally, the usefulness of this assay was further demonstrated by its suitability for measuring kinetic parameters. Table 1 shows the apparent Michaelis–Menten constants for the primer $HA_4$, UDP-GlcUA, and UDP-GlcNAc. In each case, the concentration of one substrate was varied while keeping the other two substrates near saturating at approximately $\geq 4K_{M,\,app}$. The $K_{M,\,app}$ values obtained for the UDP sugars are comparable to previously published values (0.66 versus 0.105 mM for UDP-GlcNAc [15] and 0.014 versus 0.020 mM for UDP-GlcUA [15]). A representative Michaelis–Menten plot for $HA_4$ is shown in Fig. 5.

This assay can also be used to measure inhibition, for example, by other UDP sugars. Substrate concentrations of less than $K_{M,\,app}$ were used to facilitate the detection of inhibition. A representative inhibition plot is shown in Fig. 6. The apparent inhibition constant ($K_{i,\,app}$) for UDP-Glc was determined to be 2.9 mM at $0.5K_{M,\,app}$ of each of the three PmHAS substrates (Table 2). Increasing the concentration of either UDP-GlcUA or $HA_4$ to $4K_{M,\,app}$, while keeping the other two corresponding substrates at $0.5K_{M,\,app}$, had no effect on the $K_{i,\,app}$ of UDP-Glc. In contrast, and as revealed in the representative Dixon plot (Fig. 7), increasing the concentration of UDP-GlcNAc to $4K_{M,\,app}$, while keeping the other two substrates at $0.5K_{M,\,app}$, increased $K_{i,\,app}$ four-fold from 2.9 to 12 mM. The fourfold increase in the observed $K_{i,\,app}$ is consistent with UDP-Glc acting as a competitive inhibitor of the UDP-GlcNAc transferase activity. As a control, it was shown that UDP-Glc did not inhibit the reactions of Eq. (2) or (3) outlined in Fig. 1. The mode of inhibition of UDP-Glc [45] and its potency (30% inhibition at 2 mM for *Streptococcus equisimilis* HAS [46]) is consistent with our observations.

In its current format, this signal decrease assay is very simple to perform. A quantified primer is not required for the routine detection of PmHAS activity in crude samples where partially digested unpurified HA is suitable. More important, this HAS assay does not require the use of expensive and hazardous radiolabeled sugars as in the non-continuous format. The use of a standard laboratory UV–Vis spectrophotometer provides a fast and continuous readout suitable for kinetic studies.

In conclusion, we have developed a rapid, continuous, and convenient three-enzyme coupled UV absorption assay for PmHAS. The assay was validated, and through a variety of control experiments its suitability for the determination of kinetic parameters, inhibition, and mechanism of this enzyme was demonstrated. This assay should prove to be invaluable for rapidly quantifying the presence of PmHAS in biological samples and during enzyme purification. In principle, this assay could also be adapted to detect and study other HASs.

## Acknowledgments

This work was supported by the Canadian Institutes for Health Research (MOP-74725 to J.S.M., M.C., and S.G.W.) and the National Institutes of Health (HL62244 and GM38060 to R.J.L.). We thank Kim Alan of the Respiratory Diseases of Livestock Research Unit (USDA–ARS National Animal Disease Center, Aimes, IA, USA) for the generous gift of *Pasteurella multocida* type A strain P-1059, and we thank Robert Laroce for modifying the pET15b vector.

## References

[1]. Toyokawa K, Harayama H, Miyake M. Exogenous hyaluronic acid enhances porcine parthenogenetic embryo development in vitro possibly mediated by CD44. Theriogenology. 2005; 64:378–392. [PubMed: 15955360]

[2]. Taylor KR, Gallo RL. Glycosaminoglycans and their proteoglycans: host-associated molecular patterns for initiation and modulation of inXammation. FASEB J. 2006; 20:9–22. [PubMed: 16394262]

[3]. Price RD, Myers S, Leigh IM, Navsaria HA. The role of hyaluronic acid in wound healing: assessment of clinical evidence. Am. J. Clin. Dermatol. 2005; 6:393–402. [PubMed: 16343027]

[4]. Yabushita H, Kishida T, Fusano K, Kanyama K, Zhuo L, Itano N, Kimata K, Noguchi MY. Role of hyaluronan and hyaluronan synthase in endometrial cancer. Oncol. Rep. 2005; 13:1101–1105. [PubMed: 15870928]

[5]. Adamia S, Maxwell CA, Pilarski LM. Hyaluronan and hyaluronan synthases: potential therapeutic targets in cancer. Curr. Drug Targets Cardiovasc. Haematol. Disord. 2005; 5:3–14. [PubMed: 15720220]

[6]. Volpi N. Therapeutic applications of glycosaminoglycans. Curr. Med. Chem. 2006; 13:1799–1810. [PubMed: 16787222]

[7]. Kelly MA, Moskowitz RW, Lieberman JR. Hyaluronan therapy: looking toward the future. Am. J. Orthop. 2004; 3(Suppl. 2):23–28. [PubMed: 15005297]

[8]. Fujishiro M, Yahagi N, Nakamura M, Kakushima N, Kodashima S, Ono S, Kobayashi K, Hashimoto T, Yamamichi N, Tateishi A, Shimizu Y, Oka M, Ogura K, Kawabe T, Ichinose M, Omata M. Successful outcomes of a novel endoscopic treatment for GI tumors: endoscopic submucosal dissection with a mixture of highmolecular-weight hyaluronic acid, glycerin, and sugar. Gastrointest. Endosc. 2006; 63:243–249. [PubMed: 16427929]

[9]. Watt JM, Swialto E, Wade MM, Champlin FR. Regulation of capsule biosynthesis in serotype A strains of *Pasteurella multocida*. FEMS Microbiol. Lett. 2003; 225:9–14. [PubMed: 12900014]

[10]. Chung JY, Wilkie I, Boyce JD, Townsend KM, Frost AJ, Ghoddusi M, Adler B. Role of capsule in the pathogenesis of fowl cholera caused by *Pasteurella multocida* serogroup A. Infect. Immun. 2001; 69:2487–2492. [PubMed: 11254611]

[11]. Wessels MR, Moses AE, Goldberg JB, DiCesare TJ. Hyaluronic acid capsule is a virulence factor for mucoid group A *Streptococci*. Proc. Natl. Acad. Sci. USA. 1991; 88:8317–8321. [PubMed: 1656437]

[12]. Jing W, DeAngelis PL. Dissection of the two transferase activities of the *Pasteurella multocida* hyaluronan synthase: two active sites exist in one polypeptide. Glycobiology. 2000; 10:883–889. [PubMed: 10988250]

[13]. Williams KJ, Halkes KM, Kamerling JP, DeAngelis PL. Critical elements of oligosaccharide acceptor substrates for the *Pasteurella multocida* hyaluronan synthase. J. Biol. Chem. 2006; 281:5391–5397. [PubMed: 16361253]

[14]. Jing W, DeAngelis PL. Analysis of the two active sites of the hyaluronan synthase and the chondroitin synthase of *Pasteurella multocida*. Glycobiology. 2003; 13:661–671. [PubMed: 12799342]

[15]. DeAngelis PL. Enzymological characterization of the *Pasteurella multocida* hyaluronic acid synthase. Biochemistry. 1996; 35:9768–9771. [PubMed: 8703949]

[16]. Itano N, Sawai T, Yoshida M, Lenas P, Yamada Y, Imagawa M, Shinomura T, Hamaguchi M, Yoshida Y, Ohnuki Y, Miyauchi S, Spicer AP, McDonald JA, Kimata K. Three isoforms of

mammalian hyaluronan synthases have distinct enzymatic properties. J. Biol. Chem. 1999; 274:25085–25092. [PubMed: 10455188]

[17]. Yoshida M, Itano N, Yamada Y, Kimata K. In vitro synthesis of hyaluronan by a single protein derived from mouse HAS1 gene and characterization of amino acid residues essential for the activity. J. Biol. Chem. 2000; 275:497–506. [PubMed: 10617644]

[18]. Tlapak-Simmons VL, Baggenstoss BA, Clyne T, Weigel PH. Puri-Wcation and lipid dependence of the recombinant hyaluronan synthases from *Streptococcus pyogenes* and *Streptococcus equisimilis*. J. Biol. Chem. 1999; 274:4239–4245. [PubMed: 9933623]

[19]. Pummill PE, DeAngelis PL. Alteration of polysaccharide size distribution of a vertebrate hyaluronan synthase by mutation. J. Biol. Chem. 2003; 278:19808–19814. [PubMed: 12654925]

[20]. Tlapak-Simmons VL, Baggenstoss BA, Kumari K, Heldermon C. Kinetic characterization of the recombinant hyaluronan synthases from *Streptococcus pyogenes* and *Streptococcus equisimilis*. J. Biol. Chem. 1999; 274:4246–4253. [PubMed: 9933624]

[21]. Kumari K, Tlapak-Simmons VL, Baggenstoss BA, Weigel PH. The *Streptococcal* hyaluronan synthases are inhibited by sulfhydryl-modifying reagents, but conserved cysteine residues are not essential for enzyme function. J. Biol. Chem. 2002; 277:13943–13951. [PubMed: 11799120]

[22]. Tlapak-Simmons VL, Kempner ES, Baggenstoss BA, Weigel PH. The active *Streptococcal* hyaluronan synthases (HASs) contain a single HAS monomer and multiple cardiolipin molecules. J. Biol. Chem. 1998; 273:26100–26109. [PubMed: 9748290]

[23]. DeAngelis PL. Molecular directionality of polysaccharide polymerization by the *Pasteurella multocida* hyaluronan synthase. J. Biol. Chem. 1999; 274:26557–26562. [PubMed: 10473619]

[24]. Stoolmiller AC, Dorfman A. The biosynthesis of hyaluronic acid by *Streptococcus*. J. Biol. Chem. 1969; 244:236–246. [PubMed: 5773295]

[25]. Malinowski NM, Cysyk RL, August EM. A filter paper assay for hyaluronic acid synthetase: application to the enzyme from Swiss 3T3 Wbroblasts. Biochem. Mol. Biol. Intl. 1995; 35:1123–1132.

[26]. Larjava H, Vaarala J, Saarni H, Penttinen R, Hopsu-Favu VK. A method for the hyaluronic acid synthetase assay in human skin. Arch. Dermatol. Res. 1982; 273:199–204. [PubMed: 6819817]

[27]. Spicer AP. In vitro assays for hyaluronan synthase. Methods Mol. Biol. 2001; 171:373–382. [PubMed: 11450251]

[28]. Gosselin S, Alhussaini M, StreiV MB, Takabayashi K, Palcic MM. A continuous spectrophotometric assay for glycosyltransferases. Anal. Biochem. 1994; 220:92–97. [PubMed: 7978262]

[29]. Ly HD, Lougheed B, Wakarchuk WW, Withers SG. Mechanistic studies of a retaining ct-galactosyltransferase from *Neisseria meningit-idis*. Biochemistry. 2002; 41:5075–5085. [PubMed: 11955055]

[30]. Fitzgerald DK, Colvin B, Mawal R, Ebner KE. Enzymic assay for galactosyl transferase activity of lactose synthetase and α-lactalbumin in puriWed and crude systems. Anal. Biochem. 1970; 36:43–61. [PubMed: 5482638]

[31]. Brodbeck U, Ebner KE. Resolution of a soluble lactose synthetase into two protein components and solubilization of microsomal lactose synthetase. J. Biol. Chem. 1966; 24:762–764. [PubMed: 5908140]

[32]. Davidson EA. SpeciWcity of pyruvate kinase. Biochim. Biophys. Acta. 1959; 33:238–240. [PubMed: 13651206]

[33]. Gill SC, von Hippel PH. Calculation of protein extinction coeYcients from amino acid sequence data. Anal. Biochem. 1989; 182:319–326. [PubMed: 2610349]

[34]. D'Auria G, Flores G, Falcigno L, Oliva R, Vacatello M, Corsaro MM, Parrilli M, Paolillo L. Hyaluronate tetrasaccharide–Cu(II) interaction: a NMR study. Biopolymers. 2003; 70:260–269. [PubMed: 14517914]

[35]. Reissig JL, Strominger JL, Leloir LF. A modiWed colorimetric method for the estimation of *N*-acetylamino sugars. J. Biol. Chem. 1955; 217:959–966. [PubMed: 13271455]

[36]. Asteriou T, Deschrevel B, Delpech B, Bertrand P, Bultelle F, Merai C, Vincent J-C. An improved assay for the *N*-acetyl-D-glucosamine reducing ends of polysaccharides in the presence of proteins. Anal. Biochem. 2001; 293:53–59. [PubMed: 11373078]

[37]. Starr CM, Masada RI, Hague C, Skop E, Klock JC. Fluorophore-assisted carbohydrate electrophoresis in the separation, analysis, and sequencing of carbohydrates. J. Chromatogr. A. 1996; 720:295–321. [PubMed: 8601197]

[38]. Calabro A, Midura R, Wang A, West L, Plaas A, Hascall VC. Fluorophore-assisted carbohydrate electrophoresis (FACE) of glycosaminoglycans. Osteoarthr. Cartil. 2001; 9:S16–S22. [PubMed: 11680680]

[39]. Gao N, Lehrman MA. Alternative sources of reagents and supplies for Xuorophore-assisted carbohydrate electrophoresis (FACE). Glycobiology. 2003; 13:1G–3G. [PubMed: 12634318]

[40]. Jackson P. High-resolution polyacrylamide gel electrophoresis of Xuorophore-labeled reducing saccharides. Methods Enzymol. 1994; 230:250–265. [PubMed: 8139500]

[41]. Weigel PH. Functional characteristics and catalytic mechanisms of the bacterial hyaluronan synthases. IUBMB Life. 2002; 54:201–211. [PubMed: 12512859]

[42]. Tlapak-Simmons VL, Baron CA, Gotschall R, Haque D, CanWeld WM, Weigel PH. Hyaluronan biosynthesis by class I *Streptococcal* hyaluronan synthases occurs at the reducing end. J. Biol. Chem. 2005; 280:13012–13018. [PubMed: 15668242]

[43]. Jedrzejas MJ. Structural and functional comparison of polysaccharide-degrading enzymes. Crit. Rev. Biochem. Mol. Biol. 2000; 35:221–251. [PubMed: 10907797]

[44]. DeAngelis PL, Oatman LC, Gay DF. Rapid chemoenzymatic synthesis of monodisperse hyaluronan oligosaccharides with immobilized enzyme reactors. J. Biol. Chem. 2003; 278:35199–35203. [PubMed: 12840012]

[45]. Pummill PE, DeAngelis PL. Evaluation of critical structural elements of UDP-sugar substrates and certain cysteine residues of a vertebrate hyaluronan synthase. J. Biol. Chem. 2002; 277:21610–21616. [PubMed: 11943783]

[46]. Tlapak-Simmons VL, Baron CA, Weigel PH. Characterization of the puriWed hyaluronan synthase from *Streptococcus equisimilis*. Biochemistry. 2004; 43:9234–9242. [PubMed: 15248781]

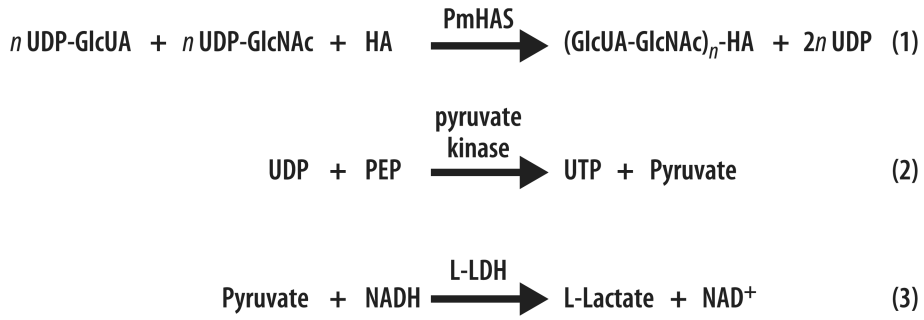


**Fig. 1.**

Schematic representation of the three-enzyme coupled signal decrease assay for PmHAS. PmHAS transfers GlcNAc and GlcUA from UDP-GlcNAc and UDP-GlcUA to the nonreducing end of HA so as to extend the HA chain. The assay relies on coupling the release of UDP produced from Eq. (1) to PEP in the presence of PK (Eq. (2)). Then pyruvate, a by-product of Eq. (2), is reduced to L-lactate with concomitant oxidation of NADH into $NAD^+$ (Eq. (3)). The decrease in NADH absorbance is monitored in a continuous fashion.

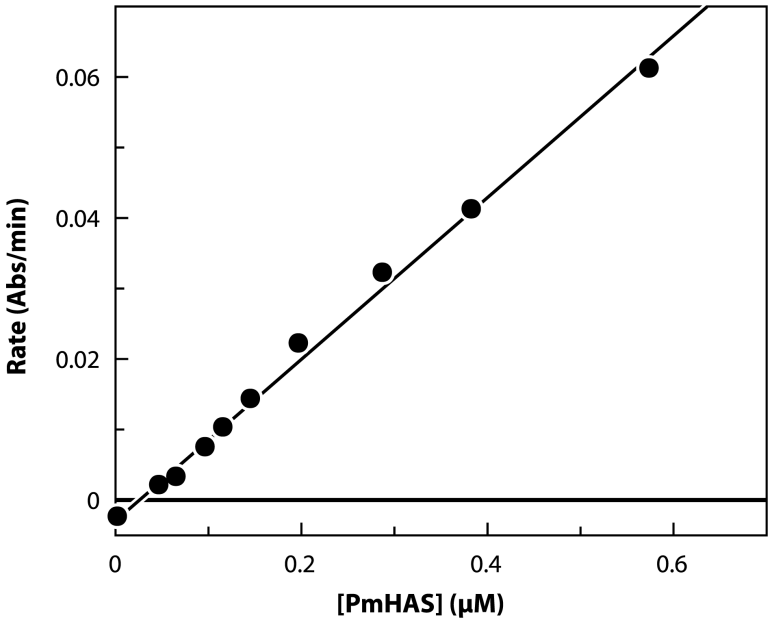


**Fig. 2.**

Detection limit for the signal decrease assay for PmHAS using purified recombinant PmHAS$^{1–703}$. Data were obtained at near-saturating conditions ($4K_{M,\,app}$) of UDP-GlcUA, UDP-GlcNAc, and $HA_4$. Absolute values of the rates are plotted. The standard deviation of repeated values is less than 10%.

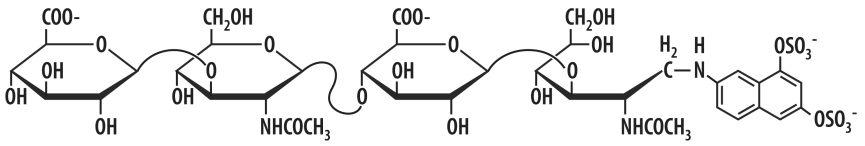


**Fig. 3.**
Structure of the Xuorescent HA primer $HA_4$-ANDA.

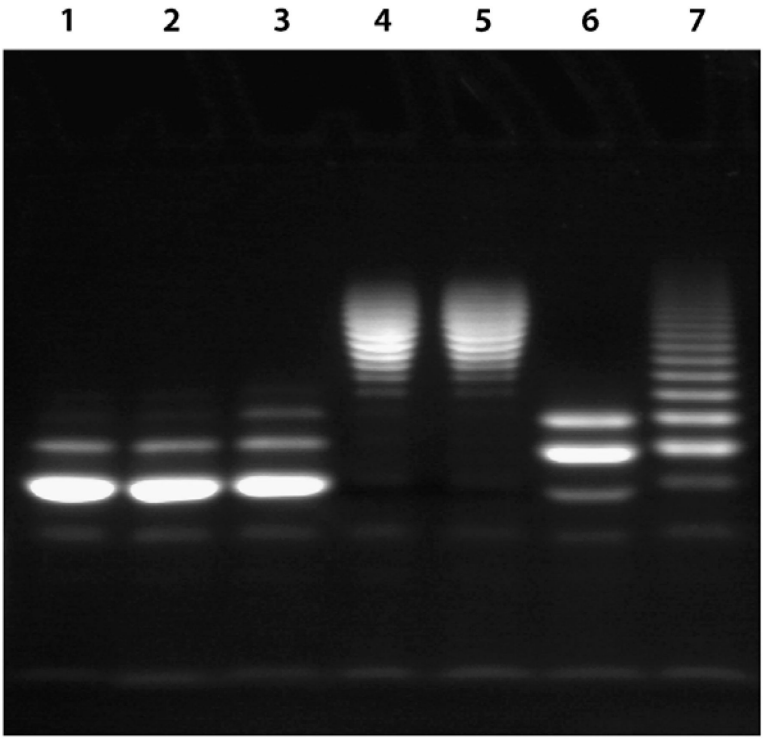


**Fig. 4.**

Fluorophore-assisted carbohydrate electrophoresis. Lane 1 contains 3 nmol of $HA_4$-ANDA and 30 nmol of both UDP-GlcNAc and UDP-GlcUA. Lane 2 contains 3 nmol of $HA_4$-ANDA. Lane 3 contains 3 nmol of $HA_4$-ANDA and 30 nmol of both UDP-GlcNAc and UDP-GlcUA in the presence of non-induced cell lysate. Lane 4 shows the extension of $HA_4$-ANDA on the addition of 3 nmol of $HA_4$-ANDA combined with 30 nmol of both UDP-GlcNAc and UDP-GlcUA in the presence of induced cell lysate. Lane 5 is a repeat of lane 4 except that the elongated $HA_4$-ANDA fragments were not treated with acid or boiled prior to loading on a gel (see Materials and methods). The elongated $HA_4$-ANDA fragment shown in lane 4 was digested with either *Streptomyces* (lane 6) or bovine testicular HAase (lane 7).

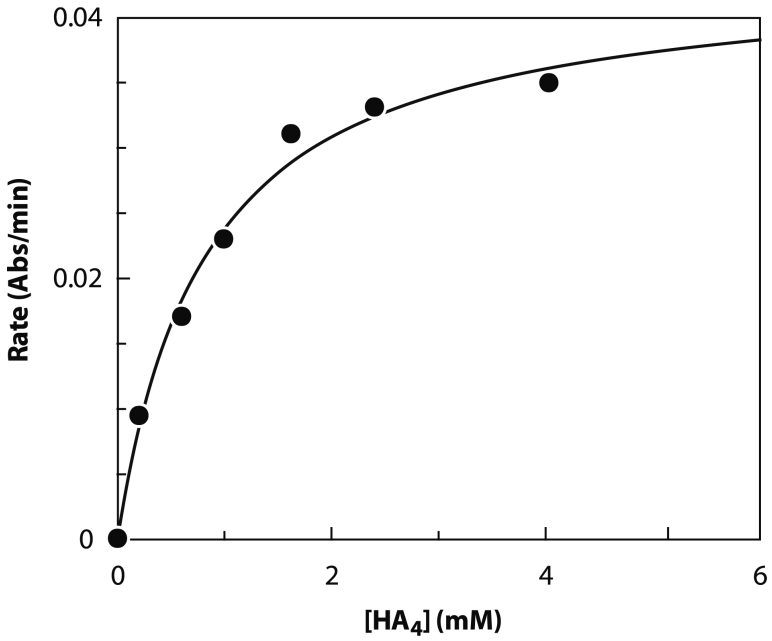


**Fig. 5.**

Representative Michaelis–Menten plot of rate (abs/min) versus [$HA_4$]. Data were obtained at near-saturating substrate concentrations (≥4$K_{M,\ app}$) for UDP-GlcUA and UDP-GlcNAc using the standard assay protocol. Absolute values of the rates are plotted.

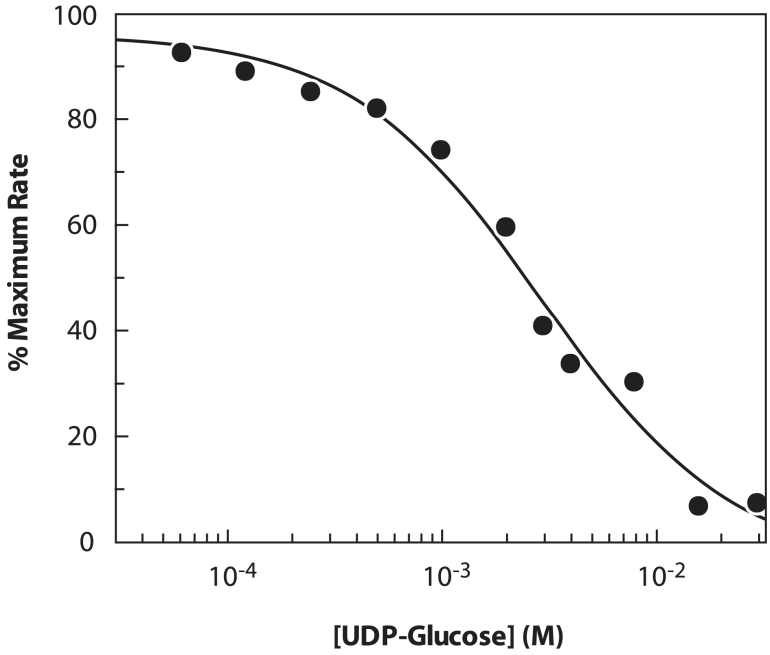


**Fig. 6.**

Representative inhibition plot for UDP-Glc obtained at $0.5K_{M,\,app}$ for each UDP-GlcUA, UDP-GlcNAc, and $HA_4$. Data were obtained using the standard assay protocol.

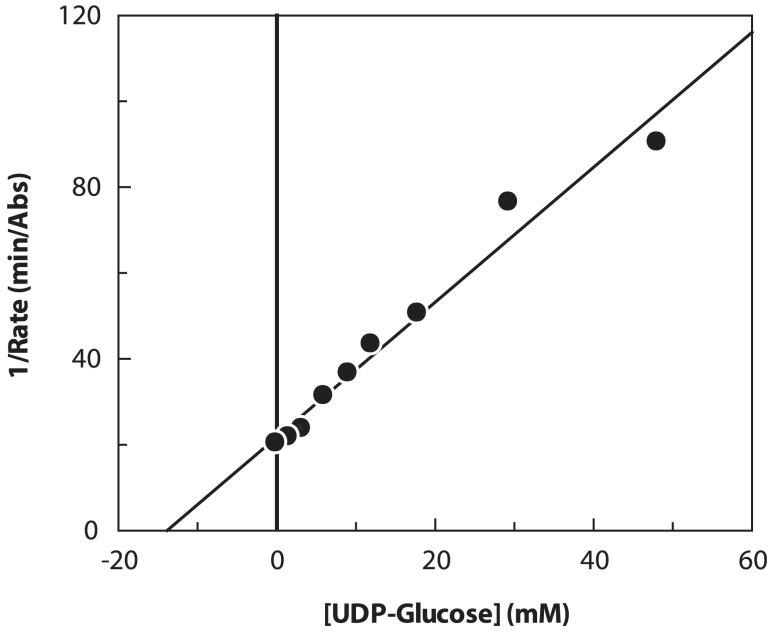


**Fig. 7.**

Representative Dixon plot of 1/rate versus [UDP-Glc]. Data were obtained at $0.5K_{M,\ app}$ for each UDP-GlcUA and $HA_4$ while working at near-saturating conditions for UDP-GlcNAc ($4K_{M,\ app}$). Absolute values of the rates are plotted.

## Table 1

Apparent Michaelis–Menten constants

| Substrate | $K_{M,\ app}$ (mM) |
|---|---|
| UDP-G1cUA | 0.014 |
| UDP-G1cNAc | 0.66 |
| $HA_4$ | 0.91 |

*Note*. Values in the table are averages of two measurements. Values were obtained using the standard assay protocol. $K_{M,\ app}$ values were obtained by varying the concentration of one substrate while keeping the other two substrates constant at near-saturating concentrations of $\geq 4K_{M,\ app}$. The reported $K_{M,\ app}$ values have errors less than 20%.

## Table 2

Inhibition of PmHAS by UDP-glucose ($K_{i, app}$, mM)

| | **[Substrate] in fold ($K_{M, app}$)** | | | |
|---|---|---|---|---|
| | $0.5K_{M, app}$ G1cNAc | $0.5K_{M, app}$ G1cNAc | $0.5K_{M, app}$ G1cNAc | $4.0K_{M, app}$ G1cNAc |
| | $0.5K_{M, app}$ G1cUA | $4.0K_{M, app}$ G1cUA | $0.5K_{M, app}$ G1cUA | $0.5K_{M, app}$ G1cUA |
| | $0.5K_{M, app}$ $HA_4$ | $0.5K_{M, app}$ $HA_4$ | $4.0K_{M, app}$ $HA_4$ | $0.5K_{M, app}$ $HA_4$ |
| UDP-G1c | 2.9 | 3.0 | 2.7 | 12 |

*Note*. Values in the table are averages of two measurements. Values listed were obtained using the standard assay protocol. $K_{i, app}$ values were determined using different substrate concentrations. Numerical values were obtained from a Dixon plot. The reported $K_{i, app}$ values have errors less than 20%.